Nano Res. 2011, 4(8): 723–728
DOI 10.1007/s12274-011-0128-7
Research Article

ISSN 1998-0124
CN 11-5974/O4

Separation of Gold Nanorods Using Density Gradient Ultracentrifugation

Shuai Li[§], Zheng Chang[§], Junfeng Liu (✉), Lu Bai, Liang Luo, and Xiaoming Sun (✉)

State Key Laboratory of Chemical Resource Engineering, Beijing University of Chemical Technology, Beijing 100029, China
[§] These authors contributed equally to this work.

Received: 17 February 2011 / Revised: 6 March 2011 / Accepted: 10 March 2011

ABSTRACT

High quality gold nanorods (NRs) with a monodisperse size and aspect ratio are essential for many applications. Here, we describe how nearly monodisperse gold NRs can be separated from polydisperse samples using density gradient ultracentrifugation. Size and dimension analysis by transmission electron microscopy (TEM) and absorption spectroscopy revealed that the Au NRs were separated mainly as a function of their aspect ratio. The surface-enhanced Raman scattering (SERS) activity of Au NRs with lower aspect ratio is notably stronger than that of NRs with higher aspect ratio under 633 nm laser excitation, due to the size-dependent absorption of the longitudinal plasmon band. The separation approach provides a method to improve the quality of NRs produced by large scale synthetic methods.

KEYWORDS

Au nanorods, aspect ratio, density gradient, separation, surface-enhanced Raman scattering (SERS)

Gold nanorods (NRs) have attracted widespread interest in both materials chemistry and biomedical science because of their special electronic, catalytic, and optical properties, and their promising applications [1–4]. For these applications, the availability of good quality monodisperse NRs with a single size and aspect ratio in large quantities is essential because their longitudinal plasmon band is highly sensitive to their aspect ratio. Electrochemical, photochemical, and seed-mediated methods have been developed for growing Au NRs in cationic surfactant aqueous solutions [5, 6]. Although significant efforts have been made to optimize the synthesis conditions, the typical, as-produced dispersions inevitably contain polydisperse gold NRs and spherical nanoparticles as by-products. The controlled preparation of NRs with a specific shape and size remains an elusive goal.

Post-synthesis separation is an efficient way to create size-uniform nanoparticles (NPs), and has recently received increasing attention [7–10]. Centrifugation has emerged as an effective method for the separation of nanomaterials with significant mass difference, and is part of routine procedures for concentrating nanoparticles or the separation of capping materials from particles [5, 11–13]. For example, small size gold spheres (< 5 nm) can be separated as a supernatant through repeated centrifugation at high speed [5]. Recently, centrifugation has been developed for efficient separation of colloidal gold NRs from a mixture of NRs and nanospheres [13]. In these cases, however,

Address correspondence to Junfeng Liu, ljf@mail.buct.edu.cn; Xiaoming Sun, sunxm@mail.buct.edu.cn

it is difficult to fine-tune the separation, especially between rods of slightly different length (or aspect ratio). Herein, we report a relatively simple and efficient method to obtain nearly monodisperse Au NRs colloids by utilizing density gradient ultracentrifugation separation (DGUS). Au NR colloidal fractions with different aspect ratio could be obtained adopting ethylene glycol aqueous solutions as density gradient media. The separated Au NRs showed size and aspect ratio dependent plasmon resonance absorption, and consequent Surface enhanced Raman scattering (SERS) activity. The latter was revealed using rhodamine 6G (R6G) as a molecular probe. Compared with previous synthesis and separation methods for NRs, this approach provides better controllability and can be used to produce monodisperse Au NRs of desired aspect ratio with narrow size distributions.

The Au NRs were prepared using a seed-mediated growth method in cetyltrimethylammonium bromide (CTAB) solutions in the presence of $AgNO_3$ [6] (see details in the Electronic Supplementary Material (ESM)). For highly efficient separation of the Au NR solution, choosing an appropriate density gradient medium is the first priority. In the DGUS method, solutions with higher density and viscosity than water (usually containing inert substances such as sucrose or CsCl) are used, resulting in enhanced differences in the sedimentation rates of NPs. Although the DGUS method has been successfully used to separate NPs of different size and shape both in aqueous and organic media [14–16], the conventional density media—including sucrose and CsCl—cannot be employed in the separation of Au NRs because they lead to significant aggregation of Au NRs. After repeated tests, ethylene glycol (EG) solutions with a suitable density distribution were chosen to prepare the density gradient, since EG solutions have appropriate capability to disperse Au NRs. In addition, CTAB was added to all the gradient solutions to further inhibit aggregation of Au NRs.

In a typical procedure, a density gradient was made by mixing different ratios of EG with aqueous CTAB solution (50%–80% of EG by volume), as labeled beside the centrifuge vessel (Fig. 1(a)). After the as-prepared Au NRs suspension (0.8 mL) was layered on top of the four-layer density gradient (50% + 60% + 70% + 80%, Fig. 1(a), tube Ⅰ) and centrifuged at 10,000 r/min (17,000 *g*) for 10 min, Au NRs were separated into distinct zones along the centrifuge tube (Fig. 1(a), tube Ⅱ). The section near the bottom of the tube was "ruby red" in color, in contrast to the upper "dark brown" parts. It is well known that the color of colloidal dispersions of gold NPs varies depending upon the shape and size of the particles. The shape-dependent color and optical properties originate from localized surface plasmons and are sensitive to their local dielectric environment. Au nanospheres have only one surface plasmon peak at about 520 nm, whereas Au NRs have both a transverse surface plasmon band at 500–550 nm and an additional longitudinal band at

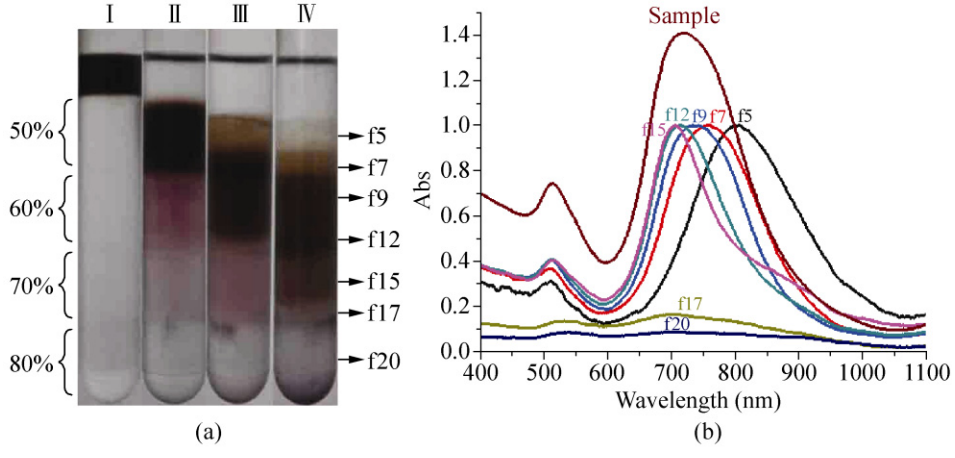

Figure 1 (a) Digital camera images of the ultracentrifuge tubes before and after separation at 10,000 r/min: (Ⅰ) before separation; (Ⅱ) after separation for 10 min; (Ⅲ) after separation for 20 min; (Ⅳ) after separation for 30 min. (b) UV–vis absorption spectra of Au NRs in typical fractions obtained from vessel Ⅳ

700–800 nm [2, 4]. The different color along the tube indicates that separation of Au NRs and NPs can be achieved in just 10 min. After centrifuging under the same conditions for longer times, the Au NRs (the brown part) could be separated further (Fig. 1(a), tubes Ⅲ and Ⅳ). Digital images of the tube Ⅱ show distinct layers along the tube, in place of the brown part in tube Ⅱ, representing further fine separation of NRs with different sizes and dimensions. Absorption spectra and transmission electron microscopy (TEM) images were recorded for Au NR fractions obtained by manual extraction at various positions along the centrifuge tube after ultracentrifugation.

Figure 1(b) shows the absorption spectra (400–1100 nm) of the original NRs solution and separated NRs in different fractions, labeled as f5–f20 in Fig. 1(a), tube Ⅳ. The original Au NRs exhibited two absorption peaks, a strong longitudinal plasmon band (LPB) at 718 nm and a weak transverse plasmon band (TPB) at 514 nm. After separation, the relative intensities of the two peaks in the absorption spectra of the NRs in fractions 5–15 remained essentially unchanged, indicating that these fractions contain mostly NRs. From the top to bottom fractions, the LPB became blue-shifted and the TPB became slightly red-shifted. It is apparent that the average aspect ratio of the NRs becomes smaller along the tube, indicating that the longer NRs settle more slowly than the shorter ones. Regarding the fractions nearer to the bottom, the TPB was red-shifted and broadened, while the relative intensity of the LPB decreased, and finally disappeared, suggesting that these fractions consist mainly of spherical particles.

TEM images showed that the original Au NRs were polydisperse with a small amount of NPs as by-product (see Fig. S-1 in the ESM). The average diameters and lengths of the NRs were 15 nm and 46 nm, respectively, giving an aspect ratio (L/d ~ 3.1). Au colloids in fractions 5–15 were nearly monodisperse NRs with a narrow size distribution (Fig. 2 and Fig. S-2 in the ESM). Fraction 17 was a mixture of fatter NRs and spherical NPs, while in fraction 20, rice-like NPs were the main product. Separation of the original gold NRs colloids has clearly been successfully achieved by the DGUS method. Size measurements were carried out on 200–500 Au NRs per sample and the average length and aspect ratio of the NRs as a function of fraction number can be clearly seen in right bottom graph of Fig. 2 (the data are also summarized in Table S-1 in the ESM). As shown in the graph, the lengths of the NRs increased with fraction number in the upper fractions while decreasing in the lower fractions, so that the NRs in fraction 12 had the maximum length. However, the increase in the diameter of the NRs led to a montonic decrease in aspect ratio with increasing fraction number. Au colloids in fraction 5 (labeled as "f5" in Fig. 2) contained NRs with an aspect ratio of ~3.8. The average aspect ratio in subsequent fractions (f7, f9, f12, f15, f17) gradually decreased from 3.5, 3.3, 3.2, 3.1 to 2.5. The distributions of lengths and aspect ratios of the separated Au NRs were narrower than those that of the original NRs (see Fig. S-2 in the ESM), demonstrating

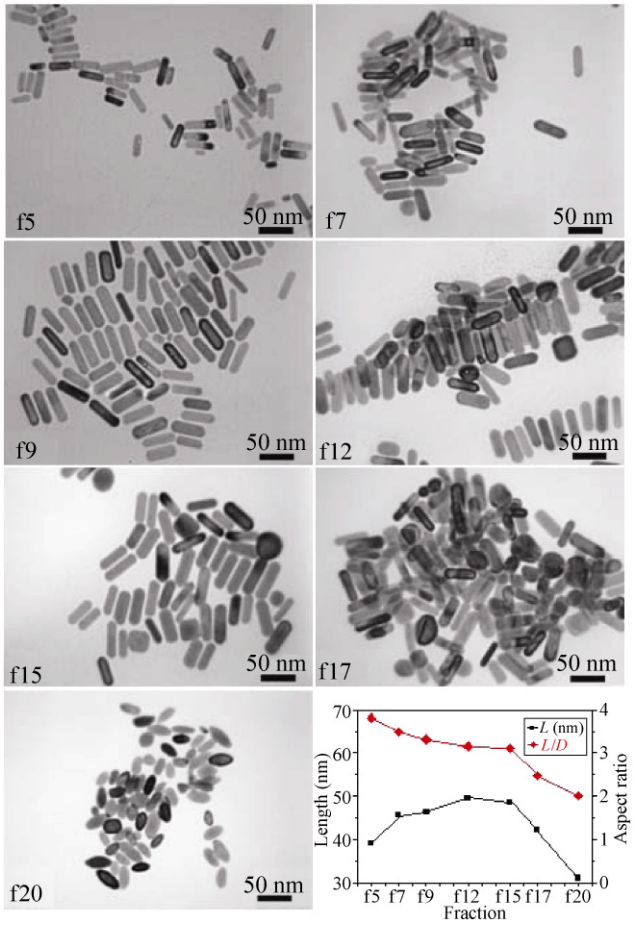

Figure 2 TEM images of separated Au NRs in typical fractions. The graph in the bottom right corner shows the evolution of the lengths (squares) and aspect ratios (triangles) in the Au NRs in different fractions (f5 means "fraction 5", and so forth)

the efficacy of the DGUS method for the separation of Au NRs into fractions with decreasing aspect ratio from the top to the bottom of the tube.

Based simply on the mass of the particles, it would be expected that longer NRs settle preferentially at the bottom of the tube, whilst shorter NRs (and nanospheres) remain at the top of the solution [17]. However, this was not the case in our separations, where shorter and fatter rods descended faster toward the bottom than longer rods with comparable or higher mass. Somewhat similar results were seen in an early study of the separation of gold NPs using a traditional centrifugation technique [2]. Au NRs with larger diameter settled faster than NRs with a smaller diameter (except in the case of f20), consistent with the theoretical prediction that the sedimentation behavior of NRs depends more strongly on the diameter of the NRs than on their total mass or aspect ratio [13]. However, in our results, rice-like gold NPs in f20 settled faster than NPs in f15, f17, which had larger diameters. This might be due to the streamlined shape of the rice-like NPs, which gives them smaller frictional resistance when moving in the density gradient solution containing CTAB. However, a detailed explanation still needs further investigation.

SERS is a powerful spectroscopic technique that can provide non-destructive and ultrasensitive characterization down to the single molecule level [18, 19]. Gold NRs have strong absorption in the near-infrared (NIR) region, and this absorption is tunable by varying the particle size and shape, which is highly desirable for many SERS applications. Therefore, it is reasonable to expect that Au NRs with different longitudinal plasmon resonances should show great differences in SERS activities. Rhodamine 6G (R6G, 10^{-6} mol/L) was adopted as a probe molecule to explore the effects of varying the aspect ratio of Au NRs. For the SERS study, a set of compact and uniform Au films were synthesized by dispersion of colloid solutions of Au NRs of varying aspect ratio onto silicon wafers. An scanning electron microscopy (SEM) image of the Au film from a solution of f9 is shown in Fig. 3(a) as an example. For practical SERS applications, signal reproducibility is of essential importance. To ensure the signal reproducibility of our samples, SERS spectra from at least five randomly selected places on the Au NRs substrate were collected under identical experimental conditions. Comparison of raw Raman and SERS spectra of R6G excited by a 633 nm laser are presented in Fig. 3(b). No Raman peaks were observed for 10^{-6} mol/L R6G in the absence of Au NRs. By simple addition of the R6G solution onto the as-synthesized Au films, immediate SERS signals were detected (curves b–d). These pronounced peaks are in good agreement with the characteristic Raman peaks of R6G described in previous work [20]. Enhancement of the Raman signals gradually increased as the aspect ratio of the Au NRs in the substrates decreased from 3.5, to 3.3 to 3.2. To further demonstrate the variation in SERS efficiency as a function of aspect ratio, the Raman peak at 1513 cm^{-1} was chosen as an example. The enhancement factors (EF) for f7, f9, and f12 using

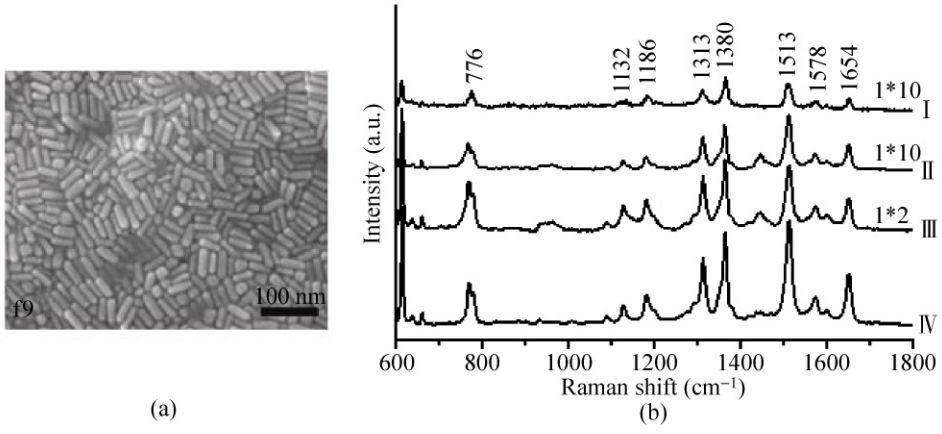

Figure 3 (a) SEM image of separated Au NRs in fraction 9; (b) Raman spectra of (Ⅰ) pure R6G (10^{-2} mol/L) and R6G (10^{-6} mol/L) in (Ⅱ) fraction 7, (Ⅲ) fraction 9, and (Ⅳ) fraction 12

10^{-2} mol/L R6G as a reference sample [21] were estimated to be about 2.2×10^4, 5.4×10^4, and 4.2×10^5, respectively. It is obvious that the Raman enhancement of Au NRs in lower fractions (e.g., f12) is better than that of upper fractions (e.g., f7). SERS measurements of R6G in Au NRs colloidal solutions showed a similar trend, confirming the relationship between SERS and aspect ratio. Such enhancement is in accord with the increasing absorbance at 633 nm from fraction f7 to f12, and agrees well with the previously reported dependence of SERS on aspect ratio [22]. Negligible spectral shifts were observed when comparing the normal Raman peaks of R6G without enhancement (curve a) and SERS peaks (curves b–d), suggesting a weak interaction between R6G and Au NRs. Therefore localized electromagnetic enhancement plays a dominant role in the enhancement [23]. The characteristic vibrational modes for CTAB were not observed in SERS spectra, as reported previously [22]. The varying SERS signal as a function of aspect ratio indicates that the Au NRs separated by the DGUS method can be used as SERS substrates with finely-tunable SERS signal intensities.

In summary, a simple method has been developed for the separation of polydisperse gold NRs based on the density gradient ultracentrifugation technique. Size and dimension analysis by TEM and absorption spectroscopy reveals that the Au NRs were separated mainly based on their aspect ratios. In addition, the SERS activity of Au NRs with lower aspect ratio was significantly stronger than that of NRs with higher aspect ratio under 633 nm laser excitation, because of the size-dependent absorption of the longitudinal plasmon band. Many previously synthesized NR samples can be regarded as mixtures of NRs with varying length and diameter, and our results suggest that discriminative separation of these NRs may lead to a new understanding of structure–property relationships for nanostructures.

Acknowledgements

This work was financially supported by the National Natural Science Foundation of China (NSFC), Beijing Natural Science Foundation (No. 2102033), the Program for New Century Excellent Talents in Universities, and the 973 Program (No. 2009CB939801).

Electronic Supplementary Material: Experimental details of the preparation, separation and characterization of the Au NRs, and TEM images, length histograms and aspect ratio histograms of Au NRs before and after separation into fractions are available in the online version of this article at http://dx.doi.org/10.1007/s12274-011-0128-7.

References

[1] Hata, H.; Kubo, S.; Kobayashi, Y.; Mallouk, T. E. Intercalation of well-dispersed gold nanoparticles into layered oxide nanosheets through intercalation of a polyamine. *J. Am. Chem. Soc.* **2007**, *129*, 3064–3065.

[2] Sharma, V.; Park, K.; Srinivasarao, M. Colloidal dispersion of gold nanorods: Historical background, optical properties, seed-mediated synthesis, shape separation and self-assembly. *Mat. Sci. Eng. R.* **2009**, *65*, 1–38.

[3] Perez-Juste, J.; Pastoriza-Santos, I.; Liz-Marzan, L. M.; Mulvaney, P. Gold nanorods: Synthesis, characterization and applications. *Coord. Chem. Rev.* **2005**, *249*, 1870–1901.

[4] Huang, X. H.; Neretina, S.; El-Sayed, M. A. Gold nanorods: From synthesis and properties to biological and biomedical applications. *Adv. Mater.* **2009**, *21*, 4880–4910.

[5] Kim, F.; Song, J. H.; Yang, P. D. Photochemical synthesis of gold nanorods. *J. Am. Chem. Soc.* **2002**, *124*, 14316–14317.

[6] Nikoobakht, B.; El-Sayed, M. A. Preparation and growth mechanism of gold nanorods (NRs) using seed-mediated growth method. *Chem. Mater.* **2003**, *15*, 1957–1962.

[7] Yao, H.; Momozawa, O.; Hamatani, T.; Kimura, K. Stepwise size-selective extraction of carboxylate-modified gold nanoparticles from an aqueous suspension into toluene with tetraoctylammonium cations. *Chem. Mater.* **2001**, *13*, 4692–4697.

[8] Wei, J. T.; Liu, F. K.; Wang, C. R. C. Shape separation of nanometer gold particles by size-exclusion chromatography. *Anal. Chem.* **1999**, *71*, 2085–2091.

[9] Jana, N. R. Nanorod shape separation using surfactant assisted self-assembly. *Chem. Commun.* **2003**, 1950–1951.

[10] Park, K.; Koerner, H.; Vaia, R. A. Depletion-induced shape and size selection of gold nanoparticles. *Nano Lett.* **2010**, *10*, 1433–1439.

[11] Wang, X.; Li, Y. D. Monodisperse nanocrystals: General synthesis, assembly, and their applications. *Chem. Commun.* **2007**, 2901–2910.

[12] Novak, J. P.; Nickerson, C.; Franzen, S.; Feldheim, D. L. Purification of molecularly bridged metal nanoparticle arrays by centrifugation and size exclusion chromatography. *Anal. Chem.* **2001**, *73*, 5758–5761.

[13] Sharma, V.; Park, K.; Srinivasarao, M. Shape separation of gold nanorods using centrifugation. *Proc. Natl. Acad. Sci. USA* **2009**, *106*, 4981–4985.

[14] Sun, X. M.; Tabakman, S. M.; Seo, W. S.; Zhang, L.; Zhang, J. Y.; Sherlock, S.; Bai, L.; Dai, H. J. Separation of nanoparticles in a density gradient: FeCo@C and gold nanocrystals. *Angew. Chem. Int. Ed.* **2009**, *48*, 939–942.

[15] Bai, L.; Ma, X. J.; Liu, J. F.; Sun, X. M.; Zhao, D. Y.; Evans, D. G. Rapid separation and purification of nanoparticles in organic density gradients. *J. Am. Chem. Soc.* **2010**, *132*, 2333–2337.

[16] Sun, X. M.; Luo, D. C.; Liu, J. F.; Evans, D. G. Monodisperse chemically modified graphene obtained by density gradient ultracentrifugal rate separation. *ACS Nano* **2010**, *4*, 3381–3389.

[17] Sun, X. M.; Zaric, S.; Daranciang, D.; Welsher, K.; Lu, Y. R.; Li, X. L.; Dai, H. J. Optical properties of ultrashort semiconducting single-walled carbon nanotube capsules down to sub-10 nm. *J. Am. Chem. Soc.* **2008**, *130*, 6551–6555.

[18] Jain, P. K.; Huang, X. H.; El-Sayed, I. H.; El-Sayed, M. A. Noble metals on the nanoscale: Optical and photothermal properties and some applications in imaging, sensing, biology, and medicine. *Acc. Chem. Res.* **2008**, *41*, 1578–1586.

[19] Zhang, J. T.; Li, X. L.; Sun, X. M.; Li, Y. D. Surface enhanced Raman scattering effects of silver colloids with different shapes. *J. Phys. Chem. B* **2005**, *109*, 12544–12548.

[20] Yang, K. H.; Liu, Y. C.; Yu, C. C. Simple strategy to improve surface-enhanced Raman scattering based on electrochemically prepared roughened silver substrates. *Langmuir* **2010**, *26*, 11512–11517.

[21] Chen, L. M.; Luo, L. B.; Chen, Z. H.; Zhang, M. L.; Zapien, J. A.; Lee, C. S.; Lee, S. T. ZnO/Au composite nanoarrays as substrates for surface-enhanced Raman scattering detection. *J. Phys. Chem. C* **2010**, *114*, 93–100.

[22] Orendorff, C. J.; Gearheart, L.; Jana, N. R.; Murphy, C. J. Aspect ratio dependence on surface enhanced Raman scattering using silver and gold nanorod substrates. *Phys. Chem. Chem. Phys.* **2006**, *8*, 165–170.

[23] Ye, W. C.; Yan, J. F.; Ye, Q.; Zhou, F. Template-free and direct electrochemical deposition of hierarchical dendritic gold microstructures: Growth and their multiple applications. *J. Phys. Chem. C* **2010**, *114*, 15617–15624.